

Design of symmetrical high-frequency coaxial wound transformer for multiport converters

Citation for published version (APA):

Waltrich, G., Duarte, J. L., & Hendrix, M. A. M. (2010). Design of symmetrical high-frequency coaxial wound transformer for multiport converters. In *Proceedings 5th IEEE Young Researchers Symposium, YRS2010, 29-30-03, Leuven* (pp. 1-7). Institute of Electrical and Electronics Engineers.

Document status and date:

Published: 01/01/2010

Document Version:

Publisher's PDF, also known as Version of Record (includes final page, issue and volume numbers)

Please check the document version of this publication:

- A submitted manuscript is the version of the article upon submission and before peer-review. There can be important differences between the submitted version and the official published version of record. People interested in the research are advised to contact the author for the final version of the publication, or visit the DOI to the publisher's website.
- The final author version and the galley proof are versions of the publication after peer review.
- The final published version features the final layout of the paper including the volume, issue and page numbers.

[Link to publication](#)

General rights

Copyright and moral rights for the publications made accessible in the public portal are retained by the authors and/or other copyright owners and it is a condition of accessing publications that users recognise and abide by the legal requirements associated with these rights.

- Users may download and print one copy of any publication from the public portal for the purpose of private study or research.
- You may not further distribute the material or use it for any profit-making activity or commercial gain
- You may freely distribute the URL identifying the publication in the public portal.

If the publication is distributed under the terms of Article 25fa of the Dutch Copyright Act, indicated by the "Taverne" license above, please follow below link for the End User Agreement:

www.tue.nl/taverne

Take down policy

If you believe that this document breaches copyright please contact us at:

openaccess@tue.nl

providing details and we will investigate your claim.

Design of Symmetrical High-Frequency Coaxial Wound Transformer for Multiport Converters

Gierr Waltrich, Jorge L. Duarte and Marcel A.M. Hendrix

Electromechanics and Power Electronics group
Department of Electrical Engineering
Eindhoven University of Technology, Eindhoven, The Netherlands
E-mail: g.waltrich@tue.nl

Abstract—A bi-directional multi-port converter can accommodate various energy storages and sources. Therefore, a multiport converter will be a good candidate for application as a future universal converter for (hybrid) electrical vehicles or local distribution systems. The main design challenge of the multiport converter analyzed in this paper is the design of its three-phase symmetrical transformer. In this converter symmetry of the leakage inductances is essential to ensure balanced three-phase currents (transferred power). These currents are interconnected by three-phase bridges which are linked together by a three-phase, three-port, transformer. To realize the equality of the leakage inductances a specific transformer design is necessary. Since conventionally wound three-phase transformer core shapes suitable for high-frequency are expensive and difficult to build, a coaxial wound transformer will be designed in this paper.

Index Terms—Coaxial, multi-port, three-phase, transformers.

I. INTRODUCTION

In (hybrid) electric vehicle applications, energy storage elements [1], e.g., battery, supercapacitor and flywheel, enable the capture and release of energy during startup and braking. A bi-directional multi-port converter can accommodate these energy storages and sources, and combine their advantages. The multi-port structure enables the bidirectional interconnection of the sources and storages to allow energy flow between the various ports, classifying as a good candidate for application as future universal converter for (hybrid) electrical vehicles or local distribution systems.

In the past decades, traditional power converter topologies have been evolving in various directions, e.g., from single-phase to multiphase interleaving, and from two-level to multilevel. Nowadays, most dc-dc power converters still deal with single-input and single-output. Recently, attention has been paid to extend the topologies to multiport converters. According to [2], two categories of integrated isolated multi-port converter are known. One type of converter involves a transformer in which there is a separate winding for each port, as shown in Fig. 1a. Therefore, all ports are fully electrically isolated. The other type has a reduced part count, with some windings absent, as illustrated in Fig. 1b, where the system allows the corresponding ports to share a common ground. However, in most applications the voltage magnitudes at each port are substantially different. For example, in renewable

energy generation systems, safe, extra low voltage batteries or supercapacitors are preferable since these lead to fewer storage units connected in series and fewer voltage balancing circuits. Adjustment of the voltage levels via the transformer turns ratio is beneficial in avoiding the device handling both high voltage and high current simultaneously.

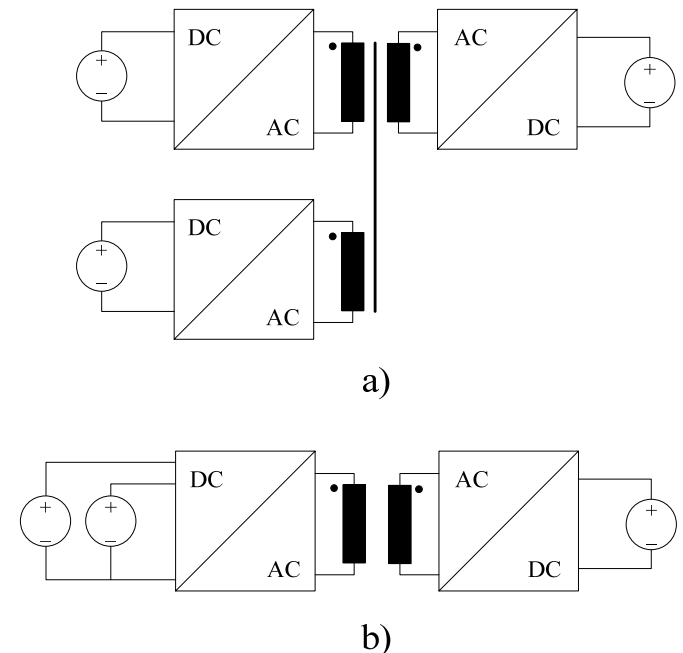


Fig. 1. Multiport converters with: a) separate winding for each port and b) windings sharing the same port.

A high-power three-port three-phase triple-active-bridge (TAB) bidirectional dc-dc converter with three separate windings has been proposed by [3], as shown in Fig. 2.

The main design challenge of the proposed high-power three-phase three-port converter is the three-phase transformer, where symmetry of the leakage inductances is essential to ensure balanced three-phase currents (transferred power). These currents are handled by three-phase bridges, which are linked together by the three-phase three-port transformer. The leakage inductances in the transformer in Fig. 2 are represented by external inductors, $L_{n A.C.}$. To realize the equality of the leakage inductances, a specific transformer design is necessary, as described in the next sections.

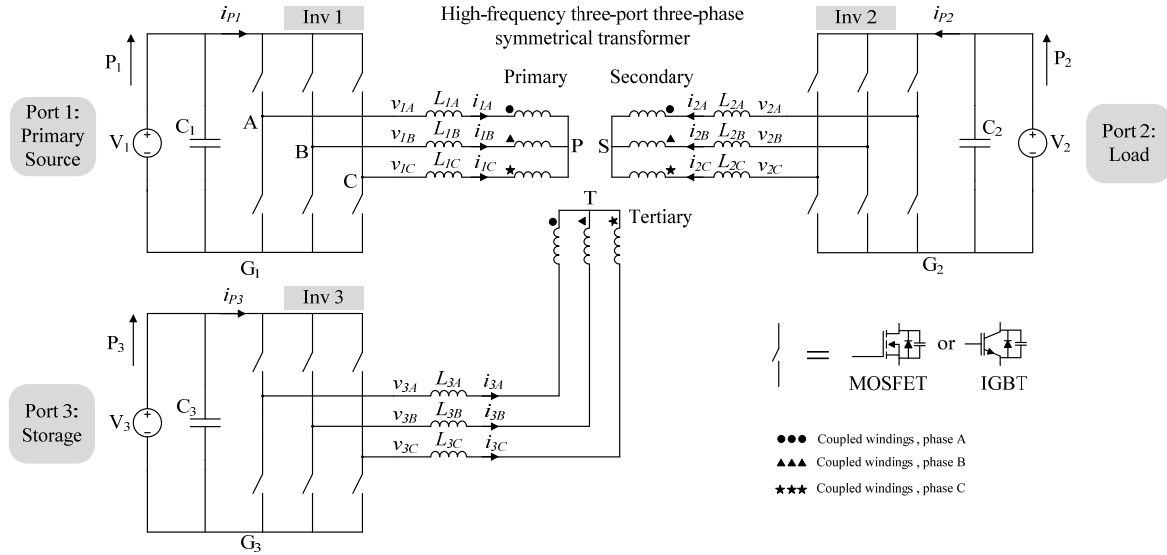


Fig. 2. High-power three-port three-phase triple-active-bridge (TAB) bidirectional dc-dc converter.

II. COAXIALLY WOUND TRANSFORMER

Transformers that can provide natural leakage symmetry are either conventionally [4] or coaxially [5] wound, as shown in Fig. 3. Since conventionally wound high-frequency three-phase transformer core shapes are expensive and difficult to build, a coaxially wound transformer is proposed in this paper. Coaxial winding techniques are commonly used in radio-frequency transformers, offering a feasible solution to confine the leakage flux within the inter-winding space. This prevents the core from being saturated locally [5]. As a result, the core and copper losses are lower, and local heating is avoided. Furthermore, from a mechanical point of view, this technique results in reduced forces within the transformer and a robust construction. In [5], it has been demonstrated that coaxial windings can lead to low loss and low leakage inductance power transformers in high-frequency soft-switched dc-dc and resonant converters. Some of the important loss aspects such as the influence of skin effect on winding resistance, the variation of core loss caused by non-uniform core flux density, and the choice of the dimensions and aspect ratios for maximum efficiency were examined in [6]. Coaxial winding techniques therefore provide a viable method for the construction of the converter transformer in Fig. 2.

As demonstrated by [3], a multi-port three-phase transformer can be thought of as three separate phases for analysis purposes. Thus, the study of only one single-phase transformer is enough in the following.

A Two windings coaxially wound transformer

To start with, the calculation of leakage inductances is considered only for two windings: the primary winding as an outer tube and an inner tube as the secondary, as shown in Fig. 4. To make the calculations easier, the secondary is considered as a solid tube.

The methodology presented in [7] was used to calculate the leakage inductance in the coaxial transformer. In Fig. 4, a

view of the coaxial cable with the magnetic field profile is shown.

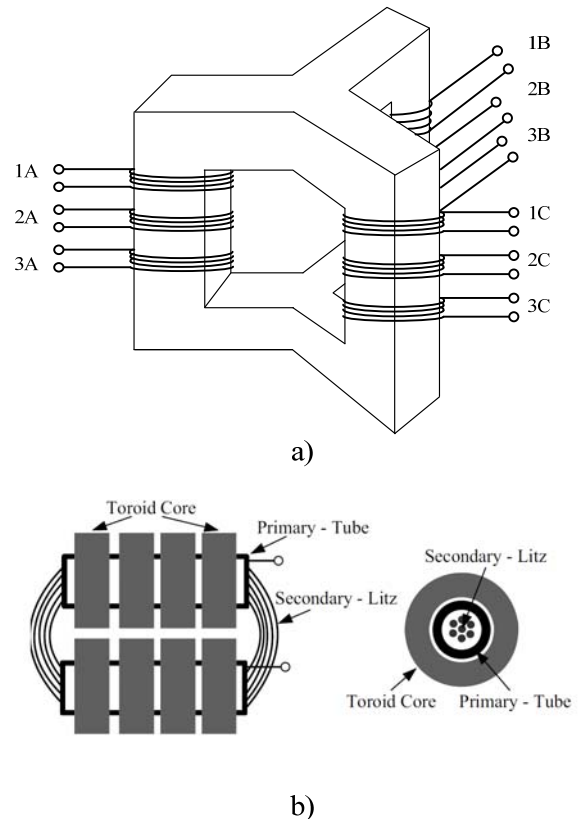


Fig. 3. Two different techniques to build multi-port transformers: a) conventionally and b) coaxially wound transformer.

To determine the total leakage inductance in Fig. 4 the calculation of the magnetic field in zones 1 to 4 is necessary. Because the cable is coaxial, in zone 4 the magnetic field is zero. By means of the magnetic field values it is possible to calculate the total energy in Fig. 4 using

$$W = \frac{1}{2} \int_{vol} \vec{B} \vec{H} d_{vol} = \frac{1}{2} L_{leak} i^2. \quad (1)$$

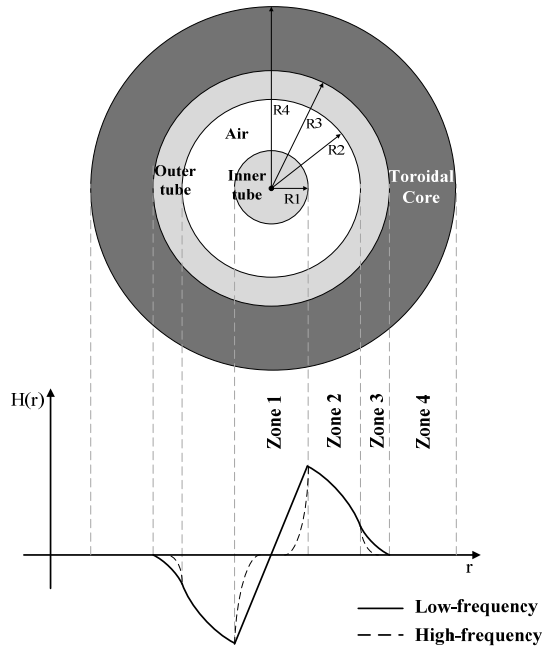


Fig. 4. Coaxial cable view with magnetic field profile, considering direct current circulating in the primary winding and this same current returning from the secondary winding.

After some mathematical manipulations the total leakage inductance per meter is found to be

$$L_{Leak} = \frac{\mu_o N^2}{2\pi} \left(\left(\frac{1}{4} + \ln \left(\frac{R_2}{R_1} \right) \right) + \left(\frac{R_3^4}{(R_3^2 - R_2^2)^2} \ln \left(\frac{R_3}{R_2} \right) + \frac{(R_2^2 - 3R_3^2)}{4(R_3^2 - R_2^2)} \right) \right) \quad (2)$$

where μ_o is the permeability of free space, which is equal to $4\pi \times 10^{-7}$ A/m, and N is the number of turns (made equal to 1 in Fig. 4). Equation (2) was developed considering direct current circulating in the primary winding and this same current returning from the secondary winding.

A 2D numerical model of the coaxial transformer in Fig. 4 was developed with Maxwell software, to calculate the energy in the four zones of the transformer. When a current with the same value in the outer tube and inner tube is imposed with opposite direction, the energy will be concentrated in the zones 1 to 3, as shown in Fig. 5. The numerical calculations confirm that the result found in (2) is correct.

If high-frequency current is used, skin effects should be considered. The magnetic field profile will change, but it can be estimated as illustrated by the dotted line in Fig. 4. Thus, to calculate the leakage inductance at high frequency, radii R_1 and R_3 must be recalculated by subtracting the skin depth as defined by

$$\delta = \sqrt{\frac{2}{\omega \sigma \mu_o \mu_{cu}}}, \quad (3)$$

where the terms ω , σ and μ_{cu} are, respectively, the angular frequency, which is equal to $2\pi f$, the conductor's conductivity, in Siemens/meter, and the relative permeability of copper.

The magnetizing inductance

$$L_{mag} = \frac{\mu_o \mu_{fe} N^2}{2\pi} \ln \left(\frac{R_4}{R_3} \right), \quad (4)$$

where, μ_{fe} is the relative permeability of the ferrite, can be

calculated considering current only in the primary (outer tube) or secondary (inner tube) winding. Therefore, all energy will be concentrated in the toroidal core, as demonstrated in Fig. 6, and only a small amount of energy will be concentrated in zones 1 to 3. However, to keep (4) simple, only the core was considered.

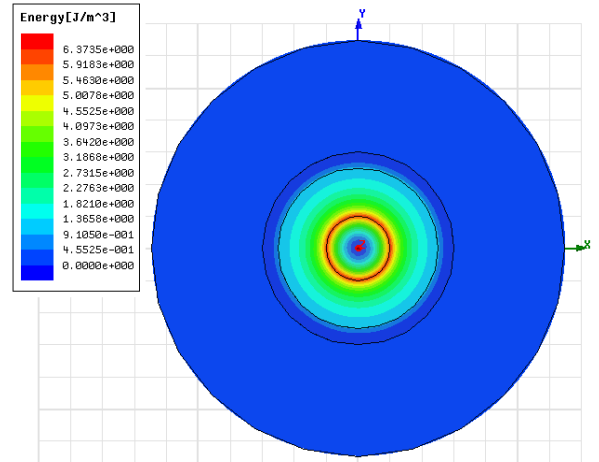


Fig. 5. 2D model, developed with Maxwell software, assuming the current in the outer and inner tubes to have the same value and opposite directions.

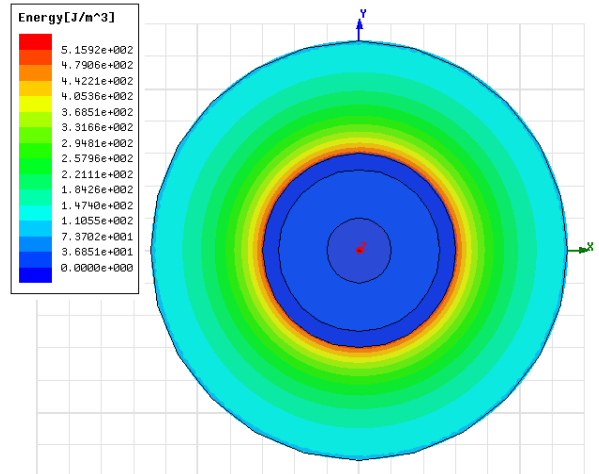


Fig. 6. 2D model, developed at Maxwell software, considering current only in the outer tube or inner tube.

Using the same procedure, as before, the magnetizing inductance observed from the secondary side was calculated, leading to the same result. Once the magnetizing and leakage inductances are known, it is possible to determine the 2 by 2 inductance matrix of this transformer.

A 3D model (Fig. 7) was also made to evaluate the fringing flux from the external cables. In the next sections an experimental set up will be build and the fringing flux will be compared with this model.

B Three windings coaxial wound transformer

The procedure explained in subsection A was repeated here, however, using three windings instead of two.

A 3 by 3 inductance matrix can be calculated. However, to obtain this matrix it is necessary to find six parameters, i.e., the magnetizing and leakage inductances observed from each side, as discussed in the next section.

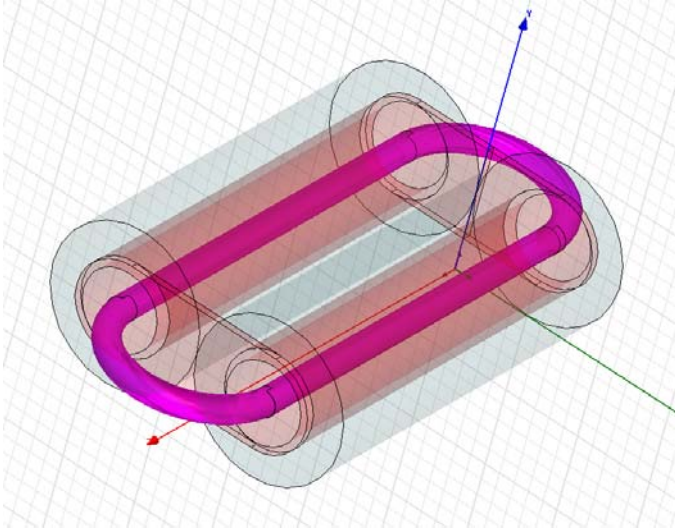


Fig. 7. 3D model from Maxwell software.

III. INDUCTANCE MATRIX

Now we have a method to calculate leakage and magnetizing inductances of a multi-port coaxial transformer, the related inductance matrix can be defined.

Based on Faraday's Law, the voltage across the terminal of a winding composed of several turns, considering the magnetic flux equal in all turns, is defined as

$$u = \sum_j \frac{d}{dt} \Phi_j. \quad (5)$$

Assuming it is composed of several windings, the voltage across a terminal winding i is described by

$$u_i = \sum_{j=1}^{N_i} \frac{d}{dt} [\Phi_{ji,1} + \Phi_{ji,2} + \dots], \quad (6)$$

where i is the number of the windings and j is the number of turns. Thus, Φ_{ji} denotes the flux through the turn j of the winding number i . The secondary index is referring to the different currents through winding 1,2,3,...

The flux Φ_{ji} is caused by the current i through the winding j , and is proportional to this current. Thus, it is possible to write a matrix, normalizing the flux to the current, as

$$\begin{bmatrix} u_1 \\ u_2 \\ \dots \end{bmatrix} = \begin{bmatrix} \sum_{j=1}^{N_1} \frac{\Phi_{j1,1}}{i_1} & \sum_{j=1}^{N_1} \frac{\Phi_{j1,2}}{i_2} & \dots \\ \sum_{j=1}^{N_1} \frac{\Phi_{j2,1}}{i_1} & \sum_{j=1}^{N_1} \frac{\Phi_{j2,2}}{i_2} & \dots \\ \dots & \dots & \dots \end{bmatrix} \frac{d}{dt} \begin{bmatrix} i_1 \\ i_2 \\ \dots \end{bmatrix}, \quad (7)$$

where the terms in the diagonal are known as measurable inductances and will be designed as L_{ij} . The others terms are mutual inductances and will be addressed as M_{ij} . Thus, the matrix can now be represented by

$$\begin{bmatrix} u_1 \\ u_2 \\ \dots \end{bmatrix} = \begin{bmatrix} L_{11} & M_{12} & \dots \\ M_{21} & L_{22} & \dots \\ \dots & \dots & \dots \end{bmatrix} \frac{d}{dt} \begin{bmatrix} i_1 \\ i_2 \\ \dots \end{bmatrix}. \quad (8)$$

It is useful to define coupling coefficients as

$$k_{ij} = \frac{M_{ij}}{\sqrt{L_{ii} L_{jj}}}. \quad (9)$$

A. Inductance matrix for two-windings transformer

Using the inductance matrix (8) it is possible to determine the terms of a π -model transformer with i windings. The inductance matrix

$$\begin{bmatrix} u_1 \\ u_2 \end{bmatrix} = \begin{bmatrix} L_1 & M \\ M & L_2 \end{bmatrix} \frac{d}{dt} \begin{bmatrix} i_1 \\ i_2 \end{bmatrix} \quad (10)$$

represents the π -equivalent circuit diagram shown in Fig. 8. In this figure we assume $M_{12}=M_{21}=M$.

The primary and secondary leakage inductance equations are defined in accordance with

$$L_{lp} = L_1 - NM \quad (11)$$

$$L_{ls} = L_2 - \frac{M}{N} \quad (12)$$

respectively, based on Fig. 8.

Because the model has 4 parameters and (10) only 3, this model is underdetermined. Some designers use this fact set the primary and secondary leakage inductance equal.

To measure the 3 parameters in (11) and (12) for a real transformer, three steps are carried out: measure the magnetizing inductance in the primary side, leaving the secondary open, short-circuit the secondary or primary side and measure the leakage from both sides and measure the magnetizing from secondary side with the primary open. Using these three steps is possible to define the components in Fig. 8.

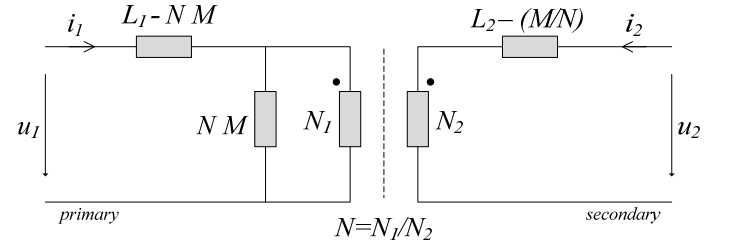


Fig. 8. Circuit diagram of π -model for a 2 winding transformer.

B. Inductance matrix for a three-windings transformer

For a three-winding transformer the inductance matrix is defined as

$$\begin{bmatrix} u_1 \\ u_2 \\ u_3 \end{bmatrix} = \begin{bmatrix} L_1 & M_{12} & M_{13} \\ M_{21} & L_2 & M_{23} \\ M_{31} & M_{32} & L_3 \end{bmatrix} \frac{d}{dt} \begin{bmatrix} i_1 \\ i_2 \\ i_3 \end{bmatrix}. \quad (13)$$

The circuit diagram for the π -model using three-winding is shown in Fig. 9.

Because the inductance matrix and circuit diagram both have 6 parameters, this system is therefore uniquely determined. The 6 parameters from Fig. 9 are found to be

$$\begin{aligned}
L_{L1} &= L_1 - \frac{M_{12}M_{13}}{M_{23}} & M &= \frac{M_{12}M_{13}}{M_{23}} \\
L_{L2} &= L_2 - \frac{M_{12}M_{23}}{M_{13}} & N_2 &= \frac{M_{23}}{M_{13}} \\
L_{L3} &= L_3 - \frac{M_{13}M_{23}}{M_{12}} & N_3 &= \frac{M_{23}}{M_{12}}
\end{aligned} \quad (14)$$

To calculate these 6 parameters in a real transformer, 6 steps must be carried out: measure 3 reflected magnetizing inductances on each side, considering the other 2 windings open, then short-circuit two windings and measure the remaining two leakage inductances for all windings.

For transformers with more than 3 windings a π -model is overdetermined. The inductance matrix can, of course, always be calculated using (8).

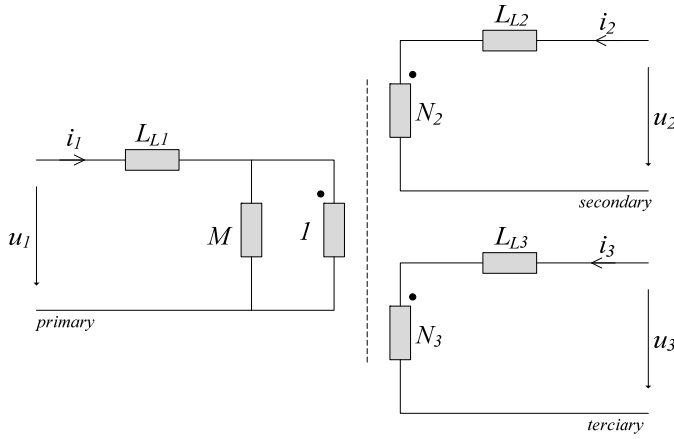


Fig. 9. Circuit diagram of the π -model for a 3 winding transformer.

IV. EXPERIMENTAL RESULTS

To check the theoretical and simulation results a simple one turn and two windings coaxial transformer prototype was constructed. Two prototypes were made: one using a tube 28.6 cm long (Fig. 10a) and another using two tubes, each with a length of 14.3 cm (Fig. 10b). Both prototypes used toroidal ferrite cores, with a relative permeability (μ_{fe}) of 700.

Results obtained from experimental measurements using an impedance analyzer are summarized in Table 1. A 3D Maxwell model was only developed for two tubes because most of leakage inductance is concentrated inside of the core, when one tube prototype is used. Thus, the fringing flux of the prototype from Fig. 10a was neglected.

Theoretical, simulation and experimental results were obtained at 10 kHz. Theory and simulation considered the skin effect.

Table 2 shows the theoretical, simulation and experimental inductance matrix of the configuration described in Fig. 10a.

Because a prototype of a coaxial transformer using three windings was not yet build, Table 2 only shows theoretical and simulation results. Since the theoretical and simulation values were very close to each other, only one 3 by 3 matrix is shown.

TABLE I
EXPERIMENTAL RESULTS FOR TWO-WINDING COAXIAL TRANSFORMER
PROTOTYPES

| | Leakage inductance (nH) | Magnetizing inductance (μ H) |
|--|--|-----------------------------------|
| Theoretical (1 tube) | 65.13 | 28.22 |
| Theoretical (2 tubes) disregarding external cables | 65.13 | 28.22 |
| 3D Maxwell software (1 tubes) | --- | --- |
| 3D Maxwell software (2 tubes) | 66.4 (internal leakage) + 31.21 (external leakage) = 96.61 | 28.34 |
| Experimental (1 tube) | 68.54 | 27.75 |
| Experimental (2 tubes) | 92.99 | 27.61 |



a)



b)

Fig. 10. Prototype coaxial transformers using: a) one tube and b) two tubes.

TABLE 2
MATRIX INDUCTANCES FOR TWO AND THREE-WINDING TRANSFORMERS.

| Two-winding transformers | | | | | | | | |
|--|--|--|--|--|--|--|--|--|
| Theoretical (μH) | | | Simulation (μH) | | | Experimental (μH) | | |
| $\begin{bmatrix} 28.22 & 28.23 \\ 28.23 & 28.30 \end{bmatrix}$ | | | $\begin{bmatrix} 28.22 & 28.22 \\ 28.22 & 28.29 \end{bmatrix}$ | | | $\begin{bmatrix} 27.46 & 27.57 \\ 27.57 & 27.75 \end{bmatrix}$ | | |
| Three-winding transformers | | | | | | | | |
| Theoretical ($\mu\text{H/m}$) | | | | Simulation ($\mu\text{H/m}$) | | | | |
| | | | | $\begin{bmatrix} 104.51 & 104.51 & 104.51 \\ 104.51 & 104.83 & 104.61 \\ 104.51 & 104.61 & 104.83 \end{bmatrix}$ | | | | |

V. CONCLUSIONS

Theoretical and simulation results were obtained for a single phase coaxial transformer which will be used on each phase of a multi-port converter proposed by [3]. Experimental results are given for one turn and two windings. The measured magnetizing and leakage inductances compare quite well with the theoretical and simulated values.

Once the dimensions of the coaxial transformer and some of its desired characteristics, e.g., number of turns and relative permeability of ferrite, are defined the leakage and magnetizing inductance can be accurately calculated.

ACKNOWLEDGEMENT

The authors gratefully acknowledge the financial support provided by the Erasmus Mundus Programme and Eindhoven University of Technology.

REFERENCES

- [1] F. Burke, "Batteries and ultracapacitors for electric, hybrid, and fuel cell vehicles," *Proc. IEEE*, vol. 95, no. 4, pp. 806–820, Apr. 2007.
- [2] Chuanhong Zhao, Round, S.D., Kolar, J.W.; "An Isolated Three-Port Bidirectional DC-DC Converter With Decoupled Power Flow Management" *Power Electronics, IEEE Transactions on*, vol. 23, Issue 5, Sept. 2008, pp. 2443 – 2453.
- [3] H. Tao, J. L. Duarte, and M. A. M. Hendrix, "High-power three-port three-phase bidirectional DC-DC converter," in *Proc. IEEE Industry Application Society Conference and Annual Meeting (IAS'07)*, New Orleans, USA, Sep. 2007, pp. 2022–2029.
- [4] R. W. DeDoncker, D. M. Divan, and M. H. Kheraluwala, "A three-phase soft-switched high-power-density DC/DC converter for high power applications," *IEEE Trans. Ind. Appl.*, vol. 27, no. 1, pp. 63–73, Jan./Feb. 1991.
- [5] M. H. Kheraluwala, D. W. Novotny, and D. M. Divan, "Coaxially wound transformers for high-power high-frequency applications," *IEEE Trans. Power Electron.*, vol. 7, no. 1, pp. 54–62, Jan. 1992.
- [6] M. S. Rauls, D. W. Novotny, and D. M. Divan, "Design considerations for high-frequency coaxial winding power transformers," *IEEE Trans. Ind. Appl.*, vol. 29, no. 2, pp. 375–381, Mar./Apr. 1993.
- [7] W. H. Hayt, "Engineering Electromagnetics", Fifth Edition, McGraw-Hill Editions, 1989, pages 387-389.